

An analysis of static and dynamic joint torques in elbow flexion-extension movements

Timotej Kodek *, Marko Munih

*Faculty of Electrical Engineering, University of Ljubljana, Slovenia Laboratory for Robotics,
Tržaška 25, 1000 Ljubljana, Slovenia*

Received 11 February 2002; received in revised form 29 April 2003; accepted 14 May 2003

Abstract

The goal of this study was to quantify shoulder, elbow and wrist dynamic and static torques in the elbow flexion-extension movements. The movements were supervised and produced by using an industrial robot manipulator that was capable of imposing a programmed arc trajectory at various velocities in the sagittal plane of the seated human subject. The muscles of the right arm being measured, were kept passive at all times of the experiment, to allow smooth guidance of the arm along a desired path.

These programmed trajectories allowed a very good motion repeatability, which is not possible in normal unconstrained movements. All four velocity and acceleration profiles were taken into account and applied to matrices describing the different dynamic components in the upper extremity motion. A range of velocities which correspond to everyday movements was tested.

The results reveal that the gravitational torque contributions have a prominent effect on the arm dynamics at low elbow velocities ($\dot{q} \approx 0.25$ rad/s). At these speeds the velocity and acceleration dependent terms can justifiably be discarded. However, at higher motion velocities ($\dot{q} \approx 1$ rad/s) the inertial and Coriolis-centrifugal contributions become non-negligible. Their effect is furthermore increased with speed and accompanied accelerations.

© 2003 Elsevier B.V. All rights reserved.

Keywords: Dynamic contributions; Static contributions; Inertial effect; Coriolis-centrifugal effect; Gravity; Human movement

Nomenclature

$B(q)$	moment of inertia matrix
$C(q, \dot{q})$	Coriolis matrix
$G(q)$	gravity vector
F_y	horizontal force component
F_z	vertical force component
F_d	dissipative coefficient matrix
F_e	elastic coefficient matrix
F_v	viscous coefficient matrix
I_i	arm segment inertia
$J^T(q)$	Jacobian matrix transpose
M_x	torque around x axis (perpendicular to the motion plane)
a_i	segment length
b_{ij}	coefficients of the inertial matrix $B(q)$
c_{ij}	coefficients of the Coriolis-centrifugal matrix $C(q, \dot{q})$
v_i	robot end effector velocity
h	vector of end effector forces and moments
l_i	segment center of gravity (COG) location
l_{hand}	hand center of gravity location
l_{handle}	rotating handle center of gravity location
m_i	segment mass
m_{fa}	forearm mass
m_{lo}	lower orthosis part mass
m_{ua}	upper arm mass
m_{uo}	upper orthosis part mass
m_{hand}	hand mass
m_{handle}	mass of rotating handle
q	joint angle vector
\dot{q}	joint velocity vector
\ddot{q}	joint acceleration vector
τ_B	inertial joint torque vector
τ_{bi}	inertial torque contribution in joint i
τ_C	Coriolis-centrifugal joint torque vector
τ_{ci}	Coriolis-centrifugal torque contribution in joint i
τ_G	gravity torque vector
τ_{gi}	gravity torque contribution in joint i
τ_p	passive moment vector
$\tau(u)$	voluntary muscle torque

1. Introduction

In movements of the human body there are many factors contributing to dynamic behavior of limbs which could be divided into two categories: (1) Firstly there are the static contributions which are present at all times such as the gravitational contributions and those arising from the specific biomechanical properties of the muscles, tendons, ligaments, and skin comprising a body segment. The latter are usually referred to as joint passive moments [1,2] and are only a function of joint angles. (2) On the other hand the dynamic contributions are in effect only when motion is in progress. The acceleration is linked to inertial contributions, while the Coriolis-centrifugal effects and viscosity relate to the joint speed of motion. Viscosity, like passive moments is an internal property of all joints in the human body whose effects are proportional to the angular speed of motion in a particular joint [3,4].

There has been a number of studies attempting to quantify the dynamic effects in human body motion, which were mostly concentrated on trajectories of the whole human body. Some studies have dealt with human locomotion [5], whereas in many other studies the dynamic effects in human rising was observed [6,7]. In the latter two studies the subject was asked to rise from a chair at various speeds at which the dynamic contributions were scrutinized, whereas the study of Pai et al. analyzed the dynamic effects of different body weight during the body rising action [8]. The dynamic effect that body motion has on the upper extremity was not studied to such an extent. Hollerbach and Flash studied the generation of various joint dynamic torques using the inverse dynamics Newton–Euler formulation in an experiment involving arm movements in the horizontal plane while holding a simple passive two degree of freedom manipulandum [9].

In the upper extremity dynamic studies there has been much work concentrated on studying angles and angular velocities, especially in the elbow and shoulder joints. The studies of Suzuki et al. and Lan have concentrated on normal reaching movements [10,11], whereas the study of Morasso studied a wide spectrum of every-day movements [12]. From all these measurements it is clearly evident that the arm joint angular velocity profiles are bell shaped. In fact the study of Zhang et al. [15] proved that the joint angle vs. time profiles, derived from point to point reaching movements can be directly scalable among different subjects independent of the motion speed. From this finding it can be deduced that the same applies also for the bell shaped velocity profiles. On the basis of the equilibrium point trajectory hypothesis, Flash derived a method for determining the magnitude of force exerted in the arm during reaching movements in the horizontal plane [13]. Similar conclusions and experimental methods can also be observed in the later work of Guomi and Kawato [14].

The study shown here is instigating the dynamic effects in the human shoulder, elbow and wrist joints in angle trajectories where the elbow is displaced through a wide range of its motion. Due to the experimental setup, where the arm is physically linked to the robot through a handle, and the robot follows the default trapezoidal velocity kinematic trajectory, the arm is also exposed to a trapezoidal joint velocity profile. Trajectories with multiple points are programmed into the robot controller in advance, meaning that the same arm trajectory can be replicated as many times as

desired. This technique with all the conditions being well defined is distinguishing this work from other studies in the field.

To get various dynamic situations during the measurement, the elbow of one subject was moved at four different speeds while following the same arc trajectories. During these actions the inertial and Coriolis-centrifugal dynamic contributions were observed and at the same time compared with the static gravity contributions.

2. Methods

2.1. Mathematical modelling

In this experimental work the human arm was described as a three degree of freedom kinematic and dynamic structure (Fig. 1).

The segment lengths are denoted with a_i , their centers of gravity (COG) with l_i while q_i indicates the positive angle directions with respect to the zero position (*dashed line*). The segment masses and inertias are presented with the m_i and I_i variables. The COG locations l_i are expressed as a distal distance from the joint marked with the same index. As in every other manipulator system, the dynamic behavior, as a relationship between applied driving torques $\tau(u)$, environment forces h and joint motion trajectories \ddot{q} , \dot{q} , q of mechanical joints can be described as [16]:

$$B(q)\ddot{q} + C(q, \dot{q})\dot{q} + G(q) + F_v\dot{q} + F_cq + F_d \operatorname{sgn}(\dot{q}) = \tau(u) - J^T(q)h. \tag{1}$$

Here q , \dot{q} and \ddot{q} represent the joint angle, angular velocity and angular acceleration vectors, which are functions of time, but were for simplicity reasons denoted with q instead of $q(t)$. They can be expressed as column vectors with indices 1, 2 and 3 referring to the shoulder, elbow and wrist respectively:

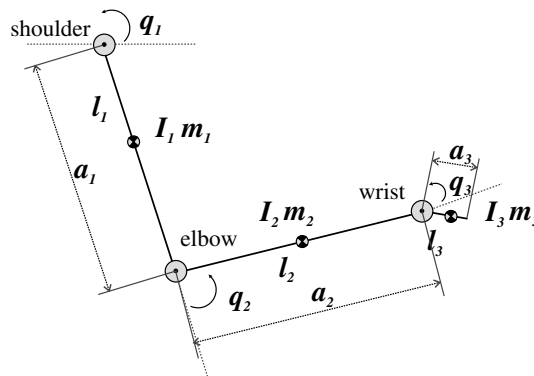


Fig. 1. Geometric definitions for the assumed human arm structure, consisting of three segments.

$$\begin{aligned}
 q &= [q_1 \quad q_2 \quad q_3]^T, \\
 \dot{q} &= [\dot{q}_1 \quad \dot{q}_2 \quad \dot{q}_3]^T, \\
 \ddot{q} &= [\ddot{q}_1 \quad \ddot{q}_2 \quad \ddot{q}_3]^T.
 \end{aligned}
 \tag{2}$$

The *moments of inertia* are represented as a (3×3) $B(q)$ matrix. The diagonal elements of the matrix represent the moment of inertia at joint i axis, while the other two joints are fixed, whereas the non-diagonal ones account for the acceleration effect of joint i on joint j . For a 3-DOF planar manipulator the inertial matrix elements were derived as follows:

$$B(q) = \begin{bmatrix} b_{11} & b_{12} & b_{13} \\ b_{21} & b_{22} & b_{23} \\ b_{31} & b_{32} & b_{33} \end{bmatrix},
 \tag{3}$$

$$\begin{aligned}
 b_{11} &= I_1 + I_2 + I_3 + l_1^2 m_1 + (a_1^2 + l_2^2) m_2 + (a_1^2 + a_2^2 + l_2^2) m_3 \\
 &\quad + 2a_1(l_2 m_2 + a_2 m_3) c_2 + 2l_3 m_3 (a_2 c_3 + a_1 c_{23}), \\
 b_{12} &= I_2 + I_3 + l_2^2 m_2 + (a_2^2 + l_3^2) m_3 + a_1(l_2 m_2 + a_2 m_3) c_2 \\
 &\quad + 2a_2 l_3 m_3 c_3 + a_1 l_3 m_3 c_{23}, \\
 b_{13} &= I_3 + l_3^2 m_3 + a_2 l_3 m_3 c_3 + a_1 l_3 m_3 c_{23}, \\
 b_{21} &= I_2 + I_3 + l_2^2 m_2 + (a_2^2 + l_3^2) m_3 + a_1(l_2 m_2 + a_2 m_3) c_2 \\
 &\quad + 2a_2 l_3 m_3 c_3 + a_1 l_3 m_3 c_{23}, \\
 b_{22} &= I_2 + I_3 + l_2^2 m_2 + (a_2^2 + l_3^2) m_3 + 2a_2 l_3 m_3 c_3, \\
 b_{23} &= I_3 + l_3^2 m_3 + a_2 l_3 m_3 c_3, \\
 b_{31} &= I_3 + l_3^2 m_3 + a_2 l_3 m_3 c_3 + a_1 l_3 m_3 c_{23}, \\
 b_{32} &= I_3 + l_3^2 m_3 + a_2 l_3 m_3 c_3, \\
 b_{33} &= I_3 + l_3^2 m_3.
 \end{aligned}
 \tag{4}$$

Multiplying this matrix with the joint accelerations \ddot{q} yields a vector of inertial contributions in all three joints $\tau_B = B(q)\ddot{q}$:

$$\tau_B = [\tau_{b1} \quad \tau_{b2} \quad \tau_{b3}]^T.
 \tag{5}$$

The second matrix, $C(q, \dot{q})$ is identifying the *centrifugal* effects in its diagonal coefficients, while non-diagonal ones account for the *Coriolis* effect induced on joint i by the velocity of joint j . For the given configuration the elements were specified as

$$C(q, \dot{q}) = \begin{bmatrix} c_{11} & c_{12} & c_{13} \\ c_{21} & c_{22} & c_{23} \\ c_{31} & c_{32} & c_{33} \end{bmatrix},
 \tag{6}$$

$$\begin{aligned}
 c_{11} &= -\{a_1[(l_2m_2 + a_2m_3)s_2 + l_3m_3s_{23}]\dot{q}_2 + l_3m_3(a_2s_3 + a_1s_{23})\dot{q}_3\}, \\
 c_{12} &= 0.5\{-2a_1[(l_2m_2 + a_2m_3)s_2 + l_3m_3s_{23}](\dot{q}_1 + \dot{q}_2) - 2l_3m_3(a_2s_3 + a_1s_{23})\dot{q}_3\}, \\
 c_{13} &= -l_3m_3(a_2s_3 + a_1s_{23})\dot{q}_{123}, \\
 c_{21} &= a_1[(l_2m_2 + a_2m_3)s_2 + l_3m_3s_{23}]\dot{q}_1 - a_2l_3m_3s_3\dot{q}_3, \\
 c_{22} &= -a_2l_3m_3s_3\dot{q}_3, \\
 c_{23} &= -a_2l_3m_3s_3\dot{q}_{123}, \\
 c_{31} &= l_3m_3[(a_2s_3 + a_1s_{23})\dot{q}_1 + a_2s_3\dot{q}_2], \\
 c_{32} &= a_2l_3m_3s_3(\dot{q}_1 + \dot{q}_2), \\
 c_{33} &= 0
 \end{aligned} \tag{7}$$

which after applying the velocity vector \dot{q} defines the joint torque dynamic contributions $\tau_C = C(q, \dot{q})\dot{q}$:

$$\tau_C = [\tau_{c1} \quad \tau_{c2} \quad \tau_{c3}]^T. \tag{8}$$

The *gravitational* contribution is expressed with a three element column vector. Every element of the τ_G vector represents the moment generated at the joint i axis as a result of the segment gravity:

$$G(q) = [\tau_{g1} \quad \tau_{g2} \quad \tau_{g3}]^T, \tag{9}$$

where

$$\begin{aligned}
 \tau_{g1} &= g_0\{[l_1m_1 + a_1(m_2 + m_3)]c_1 + (l_2m_2 + a_2m_3)c_{12} + l_3m_3c_{123}\}, \\
 \tau_{g2} &= g_0[(l_2m_2 + a_2m_3)c_{12} + l_3m_3c_{123}], \\
 \tau_{g3} &= g_0l_3m_3c_{123}.
 \end{aligned} \tag{10}$$

In these equations the following abbreviations were used: $c_1 = \cos(q_1)$, $c_{12} = \cos(q_1 + q_2)$, $c_{123} = \cos(q_1 + q_2 + q_3)$ and $s_1 = \sin(q_1)$, $s_{12} = \sin(q_1 + q_2)$, $s_{123} = \sin(q_1 + q_2 + q_3)$. While the individual segment lengths a_i were determined before a particular measurement from IR markers used by a 3D positioning system, the masses m_i , transversal segment inertial values around the COGs I_i and COG locations l_i , were obtained from the literature [17]. The gravitational acceleration g_0 was taken to be 9.81 m/s². The values used are given in Table 1.

The connection between the human hand and the robot handle (see Section 2) creates a closed chain kinematic linkage. Thus, the end effector connection is described as a three dimensional vector with its horizontal and vertical forces (F_x, F_z) and the moment around the axis perpendicular to the plane of motion (M_y) (2):

$$h = [F_x \quad F_z \quad M_y]^T. \tag{11}$$

It should be noted that h is also a function of time. These forces have to be transformed to the joint space with the Jacobian matrix $J^T(q)$ as seen in Eq. (1).

The viscous contribution of the system is expressed with the term $F_v\dot{q}$. F_v is a 3 × 3 diagonal matrix of viscosity coefficients. $F_d \operatorname{sgn}(\dot{q})$ indicates the dissipative torques

Table 1

The values of parameters m_i , l_i and I_i as estimated from the literature [17] and segment lengths a_i as measured during the experiment

m_1 [kg]	2.09
m_2 [kg]	1.25
m_3 [kg]	0.75
l_1 [m]	0.19
l_2 [m]	0.12
l_3 [m]	0.08
I_1 [kg m ²]	0.005
I_2 [kg m ²]	0.001
I_3 [kg m ²]	0.006
m_3 [kg]	0.75
a_1 [m]	0.32
a_2 [m]	0.25
a_3 [m]	0.09

with F_d being a 3×3 diagonal matrix. In the literature this product is usually denoted as the static friction torque [16]. Finally, the passive elastic torque contributions in a particular joint are expressed with the product $F_e q$, where F_e is a 3×3 diagonal matrix with the elements expressing the elasticity coefficients of every single joint.

The next observation concerns the term $\tau(u)$ in Eq. (1). The joint muscle activity is expressed in terms of the active contribution $\tau(u)$, which is in general, a function of muscle activation u . Because the subject was instructed, before the experiment, to induce no voluntary muscle action, an assumption was made:

$$\tau(u) \approx 0. \quad (12)$$

To verify if this was justified, the EMG of a typical elbow flexion-extension was recorded prior to the large batch of experiments, to access the difference between active contribution of the person and inactivity. The surface electrodes were placed on the four major flexion and extension muscles by a skilled professional (i.e. *biceps* long and short head, *triceps* and *brachioradialis*). It was evident that no EMG activity in those muscles contributing to the movement was present. Due to lack of space this is not shown in this presentation.

2.2. Measurement

In the current experiment a positionally controlled anthropomorphic 6-DOF industrial robot (*Yaskawa*[®] *MOTOMAN sk6*) was used for imposing a linear movement trajectory into the human arm in the sagittal plane (Fig. 2). A bicycle-like circular, rubber coated aluminium handle was mounted on top of the sensor in such a way, that rotation around the y axis was freely allowed. The next element in the system was a bus passenger seat, equipped with additional straps as evident from Fig. 2. The plane of motion was perpendicular to the ground and fully aligned with the sagittal plane of the subject. The subject was asked to keep his muscles relaxed at all times, while resting the arm on the handle.

$$\begin{aligned}
 m_3 &= m_{\text{hand}} + m_{\text{handle}}, \\
 l_3 &= \frac{l_{\text{hand}}m_{\text{hand}} + l_{\text{handle}}m_{\text{handle}}}{m_{\text{handle}} + m_{\text{hand}}}.
 \end{aligned}
 \tag{13}$$

In all measurements the elbow angle was moved linearly through a large portion of its motion range, while the shoulder was fixed at approximately -68° . The wrist was allowed to move freely, since the deviation from the neutral position ($q_3 = 0$) was found to be very small. All together four sets of measurements at various robot end effector velocities were made ($v_1 = 0.375$ m/s, $v_2 = 0.25$ m/s, $v_3 = 0.125$ m/s and $v_4 = 0.1$ m/s) resulting in elbow angular velocities of approximately $|\dot{q}_{21}| \approx 1$ rad/s, $|\dot{q}_{22}| \approx 0.65$ rad/s, $|\dot{q}_{23}| \approx 0.3$ rad/s and $|\dot{q}_{24}| \approx 0.25$ rad/s respectively.

The shoulder angle was kept constant by programming an appropriate arc trajectory for the subject, using no additional fixation mechanisms (Fig. 3).

The 3D tracking system *Optotrak*[®] was used to record precisely the movements of the arm during the experiment. The IR markers were attached to the skin above the rotation points of the three arm joints in consideration, to the handle and also to robot manipulator joints to allow for later verification and complete reconstruction of the measurement. The marker data was sampled at a frequency of 50 Hz, which is enough for recording human joint movements that are well within 10 Hz. All data processing was performed off-line using Matlab[®]. To remove the noise contribution, the *Optotrak*[®] sensor data was low-pass filtered at 8 Hz using a sixth order Butterworth filter provided by the Matlab[®] Signal Processing toolbox.

One healthy right-handed male who never suffered from any kind of neuromuscular disease was tested in the process (mass 77 kg, age 25) after an institutional approval. He was asked to sit in a chair, lightly grip the robot attached handle with his right arm and not exert any voluntary muscle action. Before the experiment at

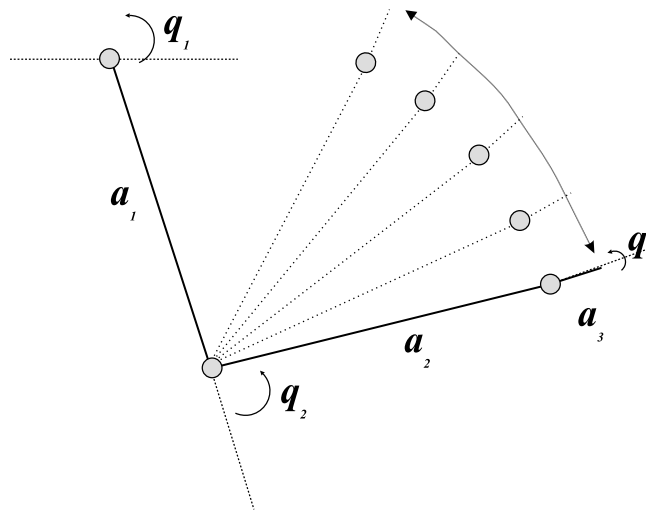


Fig. 3. The programmed elbow trajectory.

least two preliminary tests movements were made to assure that the programmed trajectory was appropriate and that the subject was comfortable. Every trial was performed under the same environmental conditions. After all these conditions were met, every one of the four different velocity trajectories was measured twice in a row. The measurement process was started with the lowest programmed speed in the first trial and later increased for every subsequent trial.

3. Results

First the repeatability of all three angle, velocity and acceleration trajectories for a typical elbow movement was analyzed. The repeatability issue indicates the capability of the apparatus and human arm to recreate the same trajectory at different times, under equal environmental conditions. For this reason six equal movement trials were recorded at the slowest trajectory with a constant elbow angular velocity of: $|\dot{q}_{21}| \approx 0.25$ rad/s (Fig. 4).

The angle standard deviations lie within ± 0.05 rad for the shoulder, ± 0.1 rad for the elbow and ± 0.2 rad for the wrist joint. When programming this trajectory it was

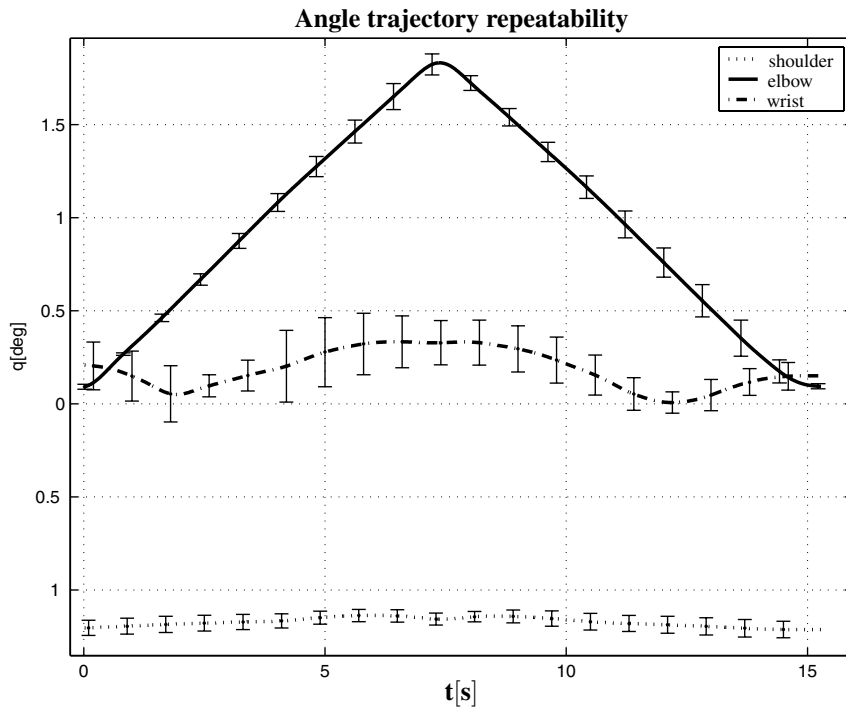


Fig. 4. Average angle trajectories with their maximum and minimum standard deviations in six consecutive same trajectory movements, where the elbow was displaced at the lowest angular velocity ($|\dot{q}_{21}| = 0.25$ rad/s).

desired to keep the shoulder and wrist angles as constant as possible. But positioning the arm fully equally at every trial was very difficult, which lead to some deviations that could be observed. The robot speed for all arm velocities was well within the operational robot speed range meaning that a similar conclusion can be deduced for all three remaining higher angular velocities ($|\dot{q}_{22}| \approx 0.3$ rad/s, $|\dot{q}_{23}| \approx 0.65$ rad/s, $|\dot{q}_{24}| \approx 1$ rad/s).

The kinematic data obtained from the four different-speed elbow joint trajectories need to be observed. The velocities were obtained by applying a simple first order difference equation to the low-pass filtered angle data, whereas accelerations were produced with the same procedure implemented on velocity trajectories (Fig. 5).

These data were used to determine particular dynamic components that contribute to human arm motion (Fig. 6). Because of a different scaling it should be noted that in both plots (Figs. 5 and 6) every row corresponds to a different velocity, the slowest being presented in the first row. With the increase of velocity the acceleration dependent inertial contribution $B(q)\ddot{q}$ and the velocity dependent Coriolis-centrifugal contribution $C(q, \dot{q})\dot{q}$ start to have a significant influence on the total joint torques (Fig. 6).

Please note that only the dynamic components change with speed, while the static gravity contribution is not a function of velocities and accelerations and therefore remains relatively constant with respect to a given angle. At low speeds the dynamic

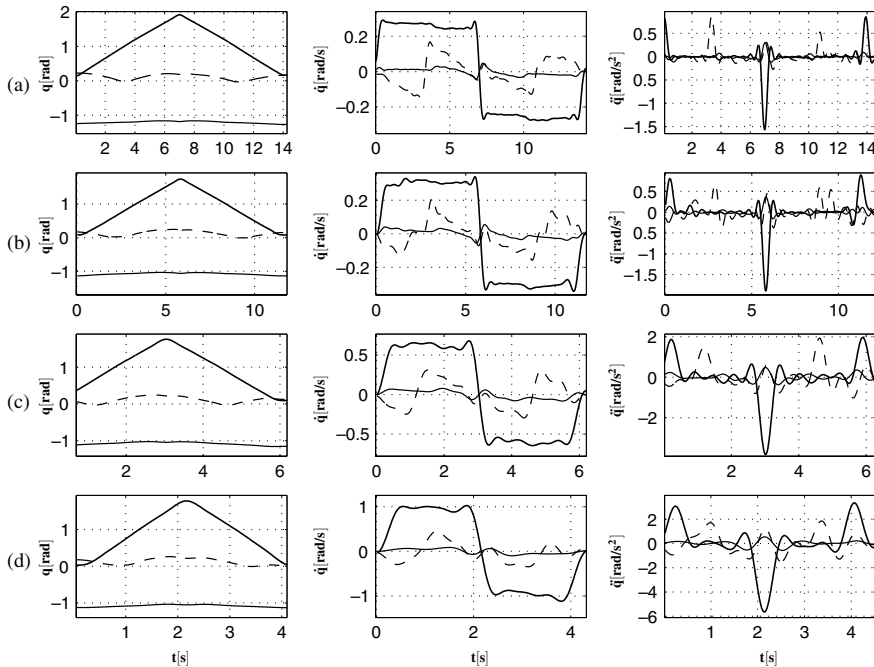


Fig. 5. Angle, velocity and acceleration profiles in all four trials when the maximum elbow angular velocities were $|\dot{q}_{21}| \approx 0.25$ rad/s (a), $|\dot{q}_{22}| \approx 0.3$ rad/s (b), $|\dot{q}_{23}| \approx 0.65$ rad/s (c) and $|\dot{q}_{24}| \approx 1$ rad/s (d) for the shoulder (thick solid), elbow (thin solid) and wrist (thin dashed) respectively.

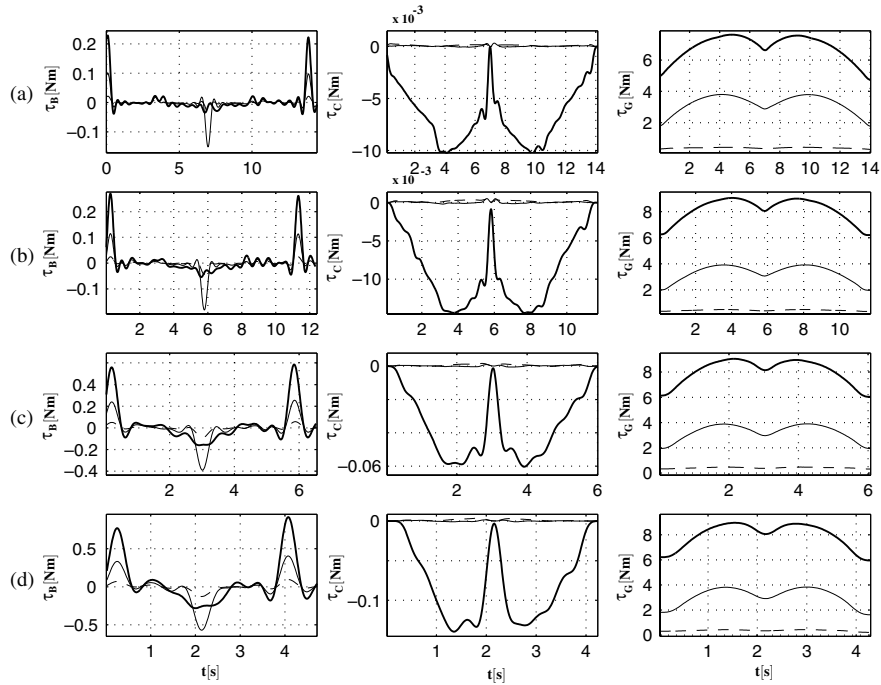


Fig. 6. The inertial, Coriolis and gravity contributions at $|\dot{q}_{21}| \approx 0.25$ rad/s (a), $|\dot{q}_{22}| \approx 0.3$ rad/s (b), $|\dot{q}_{23}| \approx 0.65$ rad/s (c) and $|\dot{q}_{24}| \approx 1$ rad/s (d) for the shoulder (thick solid), elbow (thin solid) and wrist (thin dashed) respectively.

contribution to motion is nearly negligible and is noticeable only at times of motion direction alterations. This effect becomes larger and can also be observed elsewhere with an increase in speed (Fig. 6).

4. Discussion and conclusion

In this paper, different dynamic and static contributions to human arm dynamics are investigated and quantified. Because the computed values of the inertial, Coriolis-centrifugal and gravity contributions directly depend on the obtained kinematic data, the repeatability of different trial angle readings is very important and had to be verified (Fig. 4). The velocity profiles generated with the robot manipulator were trapezoidal, which is in contrast with every-day action, bell-shaped velocity trajectories [10–12,15] (Fig. 5). After obtaining angular velocities and accelerations of particular joints all the kinematic data were applied to Eqs. (4), (7) and (10) respectively. As an outcome, the contributions of the two dynamic and one static term are shown separately (Fig. 6).

In this study only trajectories of the elbow joint were inspected. In ideal conditions the shoulder and wrist should not have any dynamic contributions to motion

but since the velocities and accelerations were non-zero (Fig. 5) this also implies non-zero dynamic contributions. The reason for using the robot manipulator for performing the described motions was that trajectories could be precisely recreated at any time while also allowing for a later complete recreation of the experiment. Nevertheless, the angle trajectories show a slightly smoother flexion-extension transition at higher velocities, which can be attributed to an increased error in positioning of the robot at higher speeds. Considering the fact that the robot movement velocities were well below the maximum possible values, the robot dynamic effects can be neglected.

It needs to be pointed out that the two dynamic contributions, which were the subject of this study (Fig. 6), are not the only dynamic components contributing to upper extremity motion. The viscosity torques $F_v\dot{q}$ from Eq. (1) also have a speed dependent effect on total torques and were not investigated in detail. The identification of $F_v\dot{q}$ exceeds the scope of this presentation and remains the topic for further investigations. The same applies for the sum of elastic and dissipative contributions $F_cq + F_d\text{sgn}(\dot{q})$, which have a considerable angle dependent effect. The viscosity and elastic contributions to motion in the upper extremity were pointed out in some other studies [1–3,18,21].

At low velocities the dynamic contributions to motion (Fig. 6(a)) are almost zero. As found, practically all studies (e.g. [1,2]) dealing with low velocity segment motions discard the dynamic contributions resulting in a substantial model simplification. Applying this fact and the fact that there are no active muscle contributions τ in the inverse dynamics upper extremity model presented in Eq. (1) leads to a very simple model representation:

$$G(q) + F_cq + F_d\text{sgn}(\dot{q}) = -J^T(q)h. \quad (14)$$

This means that the arm dynamics at low velocities is only influenced by the sum of gravitational effects $G(q)$ and passive moments which include elastic muscle and tissue contributions (F_cq) and velocity dependent dissipative effects to motion ($F_d\text{sgn}(\dot{q})$). Deducing from Fig. 6 we think it could be said that such joint velocities should not exceed 0.3 rad/s. At higher speeds the dynamic effects become considerable and are in proportion with the increase in angular velocities and accelerations. The inertial contribution vectors (Fig. 6—column 1) show the highest values at points of movement direction alterations whereas the Coriolis-centrifugal contributions (Fig. 5—column 2) play a much more significant role in the elbow joint than in the adjacent joints. This arises from the elbow angular velocities \dot{q} (Fig. 5—column 2) being much larger than the velocities of other two joints.

Because the computation of the inertial and Coriolis-centrifugal contributions are directly dependent on the derived velocities and accelerations, the method used for this derivation plays a significant role. The differentiation method utilized here is straightforward, using a low-pass Butterworth filter with an 8 Hz bandwidth frequency and a first order numerical derivative. It also needs to be emphasized that the bandwidth frequency significantly influences the results, especially the acceleration computations. The bandwidth was chosen after examining the amplitude spectrum of the angle, velocity and acceleration profiles.

The maximal elbow velocity trajectory $|\dot{q}_{24}| \approx 1$ rad/s from this study is comparable to everyday normal arm movements such as eating or reaching [10–14]. According to the results presented in Fig. 6 the contribution of dynamic terms $B(q)\ddot{q}$ and $C(q, \dot{q})\dot{q}$, in the fast movements is already considerable but still far smaller in comparison with the static gravity contribution. Although the velocity profiles in this study are not bell-shaped the computed contributions still give a reliable insight into torques during every-day actions.

Owing to the fact that the planar model structure is mathematically far less complex to describe than any other alternative, some studies suggest that the motor control system in the human brain actually uses a simplified version of such a model in determining the inverse dynamics problem [19]. In the model used in this study, the segments are presumed to be rigid, while the joints include pure rotation without any translation, which by itself is already a source of error. Apart from that, the shoulder complex also includes two translational degrees of freedom. The study of Veeger et al. [20] shows that the flexion-extension rotational center translation of the glenohumeral joint was within just 4 mm of the geometric center, making our presumption reasonably justified.

A very important issue that we have to be aware of are also anthropometric parameters from the literature [17] (Table 1) used for calculating the $B(q)$, $C(q, \dot{q})$ and $G(q)$ matrices. Masses (m_i), inertial moments (I_i) and COGs (l_i) were obtained by means of regressive equations based on body mass and height. Discrepancies in the estimation of these parameters directly influence coefficients of matrices $B(q)$, $C(q, \dot{q})$ and $G(q)$ as derived in Eqs. (4), (7) and (10). From these equations it can be observed that erroneous estimates of the anthropometric parameters (m_i , l_i , I_i) directly affect the results. However the COG (l_i) quadratically influences the inertial moments (Eq. (4)) just like the segment length a_i . Since the segment lengths were directly measured they can be considered a much more reliable quantity and are presumably not a major error source. It is quite impossible to estimate exactly the errors due to wrong parameter estimates from a literature study [17] which analyzed a population of 100 young male subjects. A further analysis dealing with the impact of parameter estimation errors on calculated torques could result in higher accuracy in the future.

Acknowledgement

This work was stimulated by the European Community project GENTLE/S—Quality of life under Framework 5.

References

- [1] H. Hatze, A three-dimensional multivariate model of passive human joint torques and articular boundaries, *Clinical Biomechanics* 12 (1997) 128–135.
- [2] A. Esteki, J.M. Mansour, An experimentally based nonlinear viscoelastic model of joint passive moment, *Journal of Biomechanics* 29 (1996) 443–450.

- [3] A.E. Engin, On the damping properties of the shoulder complex, *Journal of Biomechanical Engineering* 106 (1984) 360–363.
- [4] C.C.A.M. Gielen, J.C. Houk, S.L. Marcus, L.E. Miller, Viscoelastic properties of the wrist motor servo in man, *Annals of Biomedical Engineering* 12 (1984) 599–620.
- [5] G. Wu, Z. Ladin, Limitations of quasi-static estimation of human joint loading during locomotion, *Medical and Biological Engineering and Computing* 34 (1996) 472–476.
- [6] T.M. Bernard, M.M. Ayoub, C.J. Lin, Effects of speed of lift on static and inertial moments at the joints, *International Journal of Industrial Ergonomics* 24 (1999) 39–47.
- [7] E.B. Hutchinson, P.O. Riley, D.E. Krebs, A dynamic analysis of the joint forces and torques during rising from a chair, *IEEE Transactions on Rehabilitation Engineering* 2 (2) (1994) 49–56.
- [8] Y. Pai, M.W. Rogers, Control of body mass transfer as a function of speed of ascent in sit-to-stand, *Medicine and Science in Sports and Exercise* 22 (3) (1989) 378–384.
- [9] J.M. Hollerbach, T. Flash, Dynamic interactions between limb segments during planar arm movement, *Biological Cybernetics* 44 (1982) 67–77.
- [10] N. Lan, Analysis of an optimal control model of multi-joint arm movements, *Biological Cybernetics* 76 (1997) 107–117.
- [11] M. Suzuki, Y. Yamazaki, N. Mizuno, K. Matsumami, Trajectory formation of the center-of-mass of the arm during reaching movements, *Neuroscience* 76 (1997) 597–610.
- [12] P. Morasso, Three dimensional arm trajectories, *Biological Cybernetics* 48 (1983) 187–194.
- [13] T. Flash, The control of hand equilibrium trajectories in multi-joint arm movements, *Biological Cybernetics* 57 (1987) 257–274.
- [14] H. Guomi, M. Kawato, Equilibrium-point control hypothesis examined by measured arm stiffness during multijoint movement, *Science* 272 (1996) 117–120.
- [15] X. Zhang, D.B. Chaffin, The effects of speed variation on joint kinematics during multisegment movements, *Human Movement Science* 18 (1999) 741–757.
- [16] L. Siciliano, B. Sciavicco, *Modeling and control of robot manipulators*, The McGraw-Hill Companies, New York, 1996.
- [17] P. de Leva, Adjustments to Zatsiorsky–Seluyanov’s segment inertia parameters, *Journal of Biomechanics* 29 (1995) 1223–1230.
- [18] A.E. Engin, S.M. Chen, Kinematic and passive resistive properties of human elbow complexon, *Journal of Biomechanical Engineering* 109 (1987) 318–323.
- [19] M. Suzuki, Y. Yamazaki, K. Matsunami, Simplified dynamics of planar two-joint arm movements, *Journal of Biomechanics* 33 (2000) 925–931.
- [20] H.E.J. Veeger, B. Yu, K. An, R.H. Rozendal, Parameters for modeling the upper extremity, *Journal of Biomechanics* 30 (1996) 647–652.
- [21] T. Kodek, M. Munih, Quantification of shoulder and elbow passive moments in the sagittal plane as a function of adjacent angle fixations, *Journal of Technology and Health Care* 11 (2003) 89–103.